Multimodal Nano-Brain-Machine-Interface for Parallel Electrochemical NeuroSignal Sensing

Mohammad Poustinchi[1] , R Greg Stacey[2] and Sam Musallam[1, 2]
[1] Electrical and Computer Engineering Department, Neural Prosthetics Laboratory, McGill University
[2] Department of Physiology, McGill University
Montreal, Canada
Mohammad.poustinchi@mail.mcgill.ca

ABSTRACT

Although the information processing in the brain is mostly done through neuron's electrical activities, there might be significant information in presynaptic neurochemicals. Recent studies suggest concurrent measurement of interrelated brain's electrical and neurochemical activity may lead to novel approaches for diagnostic and better understanding of brain operation which may result in improved solutions for nervous system related disease and developing optimal neural prosthetics. We present a energy efficient multimodal CMOS Nano-Brain-Machine-Interface for simultaneous measurement of Action Potential (AP) and neurotransmitter concentration. It consist of a nano-power neural amplifier for action potential detection and amplification; a nano-power current conveyor potentiostat which senses picoscale to microscale current that corresponds to micromolar neurotransmitter concentration; and a micro-power ∑Δ Analog to Digital Convertor (ADC) to convert the analog signal (AP or neurotransmitter concentration) to digital code. This microsystem is fabricated in CMOS 0.18 µ technology and tested using recorded signals from dorsal premotor cortex (PMd) area of a macaque monkey in our lab.

Keywords: **nano-brain-machine-interface, action brain bio-signal measurement, power efficient, current conveyor, neural amplifier, analog to digital convertor**

1 INTRODUCTION

Electrical energy and chemical impulses are essential for communication throughout the nervous system. Understanding how this communication occurs gives us a better perceptive of the processes that are interrupted by neurological disorders which are the fastest-growing disease worldwide [1]. The communication in the nervous system occurs when one neuron is exited. It fires what is called an Action Potential (AP) which is a brief electrical charge travels down the axon to the synaptic terminal. The communication between two neurons begins at the microscopically small space which separates the axon from adjacent neurons. This is called the synaptic gap. The AP triggers the release of neurotransmitters which are sent through this gap to defuse to receptors on the target neuron in order to complete the transfer of the information [2].

Although the majority of studies focus on action potentials (AP) [3,4,5], however, since neurotransmitters and APs are interrelated, simultaneous measurement of both elements and investigating possible correlations might lead to better understanding of brain operation and result in improved solutions for nervous system related disease [6,7,8]. Thus a neural interface should not only detect the action potentials but also measure the neurochemical concentrations in synaptic areas, as shown in Fig. 1.

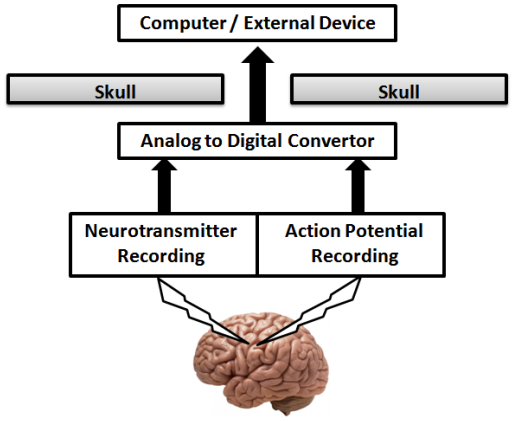

Figure 1: System level block diagram of a Action Potential and Neurotransmitter measuring interface.

Since one of our ultimate goals is to apply this neural interface in an implantable neural prosthetic; microsystems's power efficiency is crucial. The system should operate on minimum power to avoid over heating the brain tissue. In addition frequent battery replacement and surgical procedures to replace the implants are unnecessary.

We start with action potential recording module, a low power neural amplifier with 63.57 dB gain and 4.6 KHz bandwidth while consuming 653 nano watts. We continue with chemical recording module, a nano-power current conveyor-potentiostat which applies Fast-scan cyclic voltammetry electrochemical technique to detect micromolar neurotransmitter concentration by sensing picoscale to microscale current. Its power dissipation is 470 nano watts which maintaining a 2.75 KHz bandwidth. We conclude this manuscript by introducing a micro-power 65.8 SNR/ 10 bit first order ∑Δ analog to digital convertor (ADC) to convert the analog signal (AP or neurotransmitter concentration) to digital codes. Its power dissipation is 88.2 micro watts while having a 1.5 KHz bandwidth.

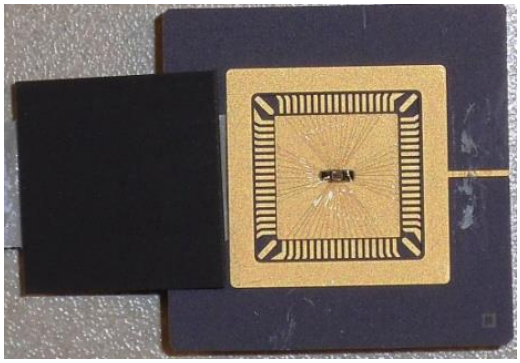

Figure 2: Electrochemical Recording and Digitizing Circuits fabricated in CMOS 0.18 um

2 ACTION POTENTIAL RECORDING CIRCUIT

Neural amplifiers are one of the major elements of an action potential recording systems. Recording of neural activity has been done using bench-top biomedical instrumentation equipment. These equipments are stationary, bulky and limited to few recording channels. Also they suffer excessive noise due to external wiring and environment. Since 1971 (Wise at Stanford) there have been remarkable efforts to miniaturize the recording systems using JFET and CMOS technology [9]. By increasing the number of recording channels, amplifier's low power dissipation is more essential than ever since each channel requires an amplifier. Several promising low power designs have been reported [9,10]. We have fabricated a neural amplifier with one of the lowest power dissipation reported to date, Table I. To design an optimum low power neural amplifier, it is important to understand the nature of action potential first. The AP's magnitude ranges between -300 to 400 uW and its bandwidth is between 0.1 to 3.5 KHz [11].

A single stage, telescopic operational amplifier fabricated in CMOS 0.18u technology, Fig. 3. The main reason of selecting this topology is its low power dissipation in addition to its high gain and input referred noise. In addition since there is no capacitor, neural amplifier area is very small. The main drawback of telescopic amplifier is its limited swing; but based on action potential range, the achieved swing is adequate. We have an on chip biasing circuitry which adds to system accuracy and mobility. The neural amplifier is design to operate in weak and moderate inversion region to minimize power dissipation. It has 63.57 dB DC Gain and 4.6 KHz bandwidth while consuming 653 nano watts. Furthermore; the amplified signal is buffered in order to drive the ADC. A source follower voltage buffer is used to prepare the amplified signal for further processing. Since we required more bandwidth in AP recording we were not able to use the amplifier used in neurotransmitter recording interface. We increase the bandwidth at the cost of slight increase in power dissipation.

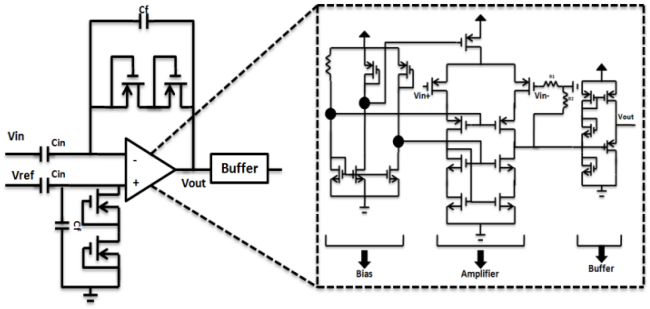

Figure 3: Overall system diagram of the low noise neural amplifier and Transistor level diagram

To validate the amplifier performance, we have used action potentials which were recorded in physiology division of our lab using chronic multi-electrode arrays in an awake, behaving male macaque monkey. Figure Fig. 4, shows 50 waveforms from one neuron in dorsal premotor cortex (PMd) area. These waveforms were recorded approximately six months after array implantation. The initial signal magnitude was between -99.4 to 39.78 uV and amplified to -0.15 to 0.06 V, Fig. 4.

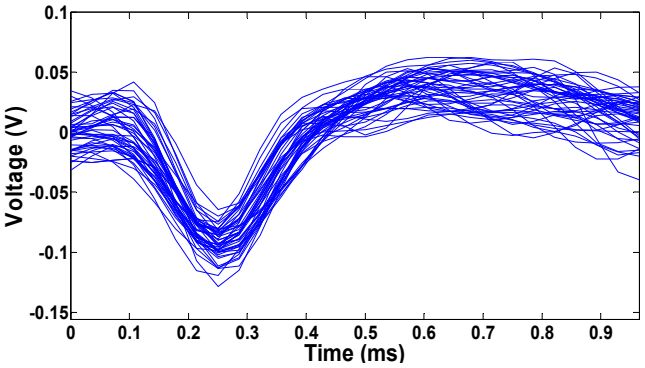

Figure 4: Recorded and amplified action potential form monkey's brain PMd

Specifications	This Work	[12]	[13]
Fabrication Year	2013	2013	2013
Technology (µ m)	0.18	0.18	0.18
DC Gain (dB)	63.57	48.36	55.9
3dB Bandwidth (KHz)	4.6	3.7	1 to 10
Phase Margin (deg)	84.45	59	63
Supply Voltage (V)	1	0.9	1
Output Swing (V)	-0.3,+0.3	-0.2,0.2	-0.3, 0.3
Power (µ W)	0.653	3.7	13

Table 1 : Low Power Neural Amplifier Specifications and Comparison.

3 NEUROTRANSMITTER RECORDING CIRCUIT

Neurotransmitters carry extremely important information which decoding this data my lead to breakthrough in understanding how neurons work and communicate in order to achieve an optimum neural prostheses. Previous studies suggest that electrochemical sensors are suitable for neurochemical sensing [14, 15].Every neurotransmitter is associated with a certain

voltage [16]. To measure neurochemical concentration, this voltage is applied between the working and reference electrode. The potential difference generates a reduction-oxidation (red-ox) current which is proportional to the neurotransmitter concentration [16]. Our goal is to implement a device that possesses high sensitivity, high chemical selectivity, and fast temporal resolution. Thus we are applying Fast-scan cyclic voltammetry technique which possesses good chemical selectivity while maintaining subsecond temporal resolution [16].

We have implemented a CMOS potentiostat, Fig.2, which consist of a current conveyor that converts pico to nano-amp red-ox current to voltage. To measure the electrochemical current, the red-ox potential is applied between working and reference electrode. The core of the current conveyor is the operational amplifier. Instead of using power hungry front end amplifiers; a wide swing folded cascade amplifier, Fig. 5, is used for its high gain and stability [12].

Power dissipation is minimized since the Op-Amp is designed to operate in the subthreshold region. We chose a folded cascode due to its high gain and low bandwidth. We have reduced the power consumption by decreasing the unity gain bandwidth.

$V_{red\text{-}ox}$ is applied across R_{Sensor}. $I_{red\text{-}ox}$ which is proportional to neurochemical concentration, accumulates charge on C_{INT} over the integration period T_{INT}.Output voltage is calculated by Equation (1). In addition since integration is an averaging operation, this circuit provides high noise immunity.

$$V_{out} = \frac{1}{C_{INT} \times R_{Sensor}} \int_0^{T_{INT}} V_{red-ox}\, dt \qquad (1)$$

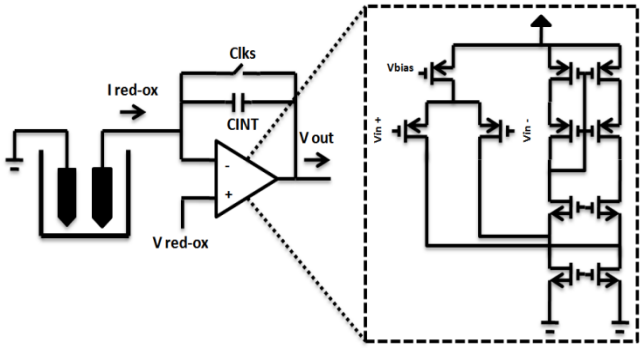

Figure 5: Overall system diagram and Transistor schematic level of the low power potentiostat

Specifications	This Work	[17]	[12]
Fabrication Year	2013	2009	2013
Technology (µ m)	0.18	0.18	0.18
DC Gain (dB)	65.1	62	48.36
Unity Gain Bandwidth (MHz)	4.75	0.54	2.408
Phase Margin (deg)	83.8	52	59
Supply Voltage (V)	1	0.9	0.9
Output Swing (V)	-0.45,+0.43	-0.2,0.2	-0.2,0.2
Power (µ W)	0.47	9.9	3.741

Table 2: Amplifier Specifications and Comparison

The designed Op-Amp consumes 470 nano Watts. This power dissipation is one of the lowest reported [12, 17]. Table II summarizes the amplifier's specifications in addition to comparing our work to other similar designs. Fig. 6 shows the measured red-ox current in response to addition of five uM Dopamine (neurotransmitter).

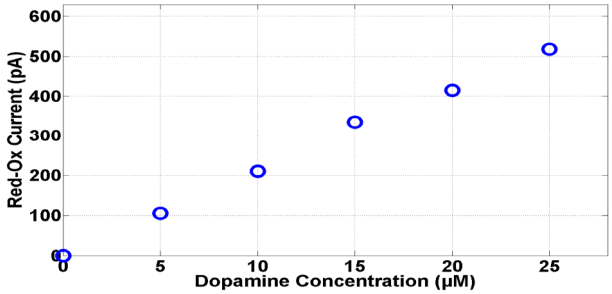

Figure 6: The static red-ox current in response to addition of 5 µM dopamine

4 10 BIT, ∑Δ DIGITIZING CIRCUIT

To convert the measured brain analog biosignal into a digital code, a 10 bit first order ∑Δ ADC is fabricated in CMOS 0.18u technology. We choose ∑Δ topology for its high resolution, low power and small area. Since brain activities are in mille second to second range, high speed digitizers are not required. ∑Δ ADC owes its performance to oversampling and noise shaping. Quantization noise is pushed out of the band of interest. It consists of an integrator followed by a quantizer in forward path and a Digital to Analog Converter (DAC) in feedback path followed by a decimator, as shown in Fig. 7.

The major design goal was minimizing the power dissipation while meeting required specifications. Thus, a lower sampling frequency was selected in addition to low power biasing. Total ADC power dissipation is 88.2 µW which is comparable with similar designs and one of the lower ones in CMOS 0.18 technology.

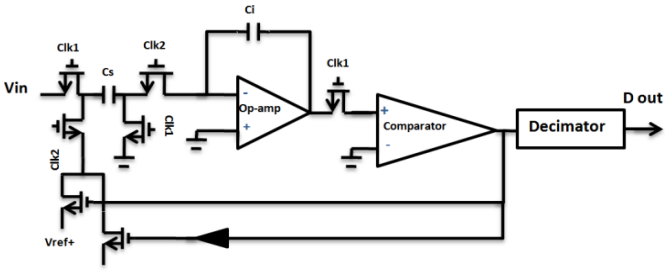

Figure 7. Overall system diagram of the ∑Δ ADC

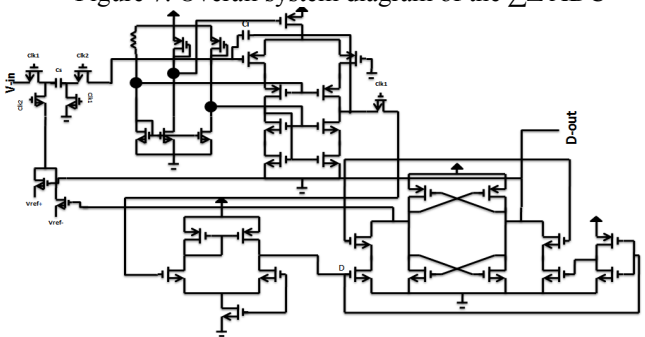

Figure 8: Transistor level diagram of the same ADC

ADC bandwidth is 1.5 KHz while sampling at 384 KHz with 65.8 dB Signal-to-Noise (SNR) ratio which is equivalent to 10 bit resolution, Equation. 2. The Oversampling Ratio (OSR) is 128. Equation. 3 Demonstrate the relationship between bandwidth, sampling frequency and oversampling ratio.

$$Bit\ Resolution = \frac{SNR(dB) - 1.76}{6.02} \quad (2)$$

$$Bandwidth = \frac{F_{sampling}}{2 \times OSR} \quad (3)$$

We tested the ADC by computing the Fast Fourier Transform (FFT) of the output to calculate the power and Signal-to-Noise-Ratio (SNR). Fig. 10 shows the power spectral density of the 10 bit first order sigma delta ADC. The total number of samples is 1024 and Over Sampling Ratio (OSR) is 128. To find the peak SNR, input amplitude swept over the input swing range, Fig. 9.

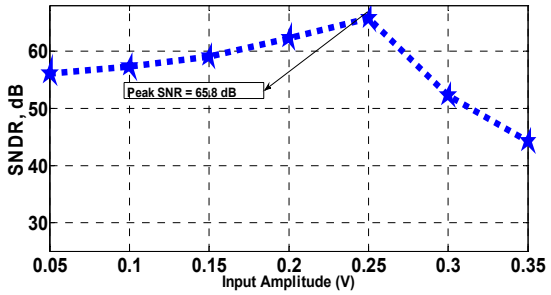

Figure 9: SNR Vs Input of the 10 bit, sigma delta ADC

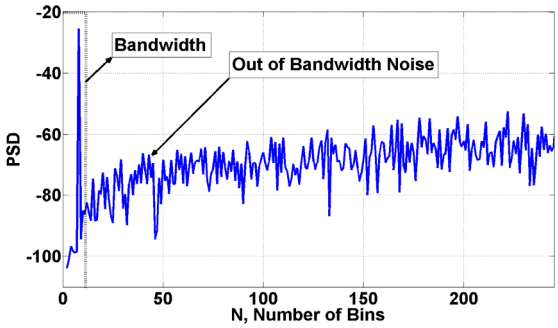

Figure 10: PSD plot for the 10 bit, sigma delta ADC

REFERENCES

[1] Remington, Patrick L., Ross C. Brownson, and Mark V. Wegner. *Chronic disease epidemiology and control*. No. Ed. 3. American public health association, 2010.

[2] Bear, Mark F., Barry W. Connors, and Michael A. Paradiso, eds. *Neuroscience*. Wolters Kluwer Health, 2007.

[3] Musallam, Sam, B. D. Corneil, Bradley Greger, Hans Scherberger, and R. A. Andersen. "Cognitive control signals for neural prosthetics." *Science* 305, no. 5681 (2004): 258-262.

[4] Hochberg, Leigh R., Mijail D. Serruya, Gerhard M. Friehs, Jon A. Mukand, Maryam Saleh, Abraham H. Caplan, Almut Branner, David Chen, Richard D. Penn, and John P. Donoghue. "Neuronal ensemble control of prosthetic devices by a human with tetraplegia." *Nature* 442, no. 7099 (2006): 164-171.

[5] Berger, Theodore W. "Implantable biomimetic microelectronics for the replacement of hippocampal memory function lost due to damage or disease." In *Neural Networks, 2004. Proceedings. 2004 IEEE International Joint Conference on*, vol. 3, pp. 1659-vol. IEEE, 2004.

[6] Lally, Níall, Paul G. Mullins, Mark V. Roberts, Darren Price, Thomas Gruber, and Corinna Haenschel. "Glutamatergic correlates of gamma-band oscillatory activity during cognition: A concurrent ER-MRS and EEG study." *NeuroImage* 85 (2014): 823-833.

[7] Donahue, Manus J., Swati Rane, Erin Hussey, Emily Mason, Subechhya Pradhan, Kevin W. Waddell, and Brandon A. Ally. "γ-Aminobutyric acid (GABA) concentration inversely correlates with basal perfusion in human occipital lobe." *Journal of Cerebral Blood Flow & Metabolism* (2014).

[8] Poustinchi, Mohammad, and Sam Musallam. "Towards an implantale intelligent CMOS neurotrophic factor delivery micro neural prosthetic for Parkinson's disease." In *Neural Engineering (NER), 2013 6th International IEEE/EMBS Conference on*, pp. 863-867. IEEE, 2013.

[9] Jochum, Thomas, Timothy Denison, and Patrick Wolf. "Integrated circuit amplifiers for multi-electrode intracortical recording." *Journal of neural engineering* 6, no. 1 (2009): 012001.

[10] Seo, Dongjin, Jose M. Carmena, Jan M. Rabaey, Elad Alon, and Michel M. Maharbiz. "Neural dust: An ultrasonic, low power solution for chronic brain-machine interfaces." *arXiv preprint arXiv:1307.2196* (2013).

[11] Hopfield, J. J. "Pattern recognition computation using action potential timing for stimulus representation." *Nature* 376, no. 6535 (1995): 33-36.

[12] Wilson, William, Tom Chen, and Ryan Selby. "A current-starved inverter-based differential amplifier design for ultra-low power applications." In *Circuits and Systems (LASCAS), 2013 IEEE Fourth Latin American Symposium on*, pp. 1-4. IEEE, 2013.

[13] Wu, C-Y., W-M. Chen, and L-T. Kuo. "A CMOS Power-Efficient Low-Noise Current-Mode Front-End Amplifier for Neural Signal Recording." (2013): 1-1.

[14] Luo, Tao, Hongyi Wang, Hongjiang Song, and Jennifer Blain Christen. "CMOS potentiostat for chemical sensing applications." In *Sensors, 2013 IEEE*, pp. 1-4. IEEE, 2013.

[15] Murari, Kartikeya, Milutin Stanacevic, Gert Cauwenberghs, and Nitish V. Thakor. "Integrated potentiostat for neurotransmitter sensing." *Engineering in Medicine and Biology Magazine, IEEE* 24, no. 6 (2005): 23-29.

[16] Poustinchi, Mohammad, and Sam Musallam. "Low power noise immune circuit for implantable CMOS neurochemical sensor applied in neural prosthetics." In*Neural Engineering (NER), 2011 5th International IEEE/EMBS Conference on*, pp. 695-699. IEEE, 2011.

[17] Pan, Sheng-Wen, Chiung-Cheng Chuang, Chung-Huang Yang, and Yu-Sheng Lai. "A novel OTA with dual bulk-driven input stage." In *Circuits and Systems, 2009. ISCAS 2009. IEEE International Symposium on*, pp. 2721-2724. IEEE, 2009.